Weierstraß-Institut
für Angewandte Analysis und Stochastik

Leibniz-Institut im Forschungsverbund Berlin e. V.

Preprint ISSN 2198-5855

Energy level alignment of confined hole states in $InAs_{1-x-y}Sb_xP_y$ double quantum dots

Karen M. Gambaryan[1], Owen Ernst[2], Torsten Boeck[3], Oliver Marquardt[4]

submitted: August 28, 2023

[1] Dept. of Physics of Semiconductors and Microelectronics
Yerevan State University
1 A. Manoukian Str.
Yerevan 0025
Armenia
E-Mail: kgambaryan@ysu.am

[2] Leibniz Institute for Crystal Growth
Max-Born-Str. 2
12489 Berlin
Germany
E-Mail: owen.ernst@ikz-berlin.de

[3] Leibniz Institute for Crystal Growth
Max-Born-Str. 2
12489 Berlin
Germany
E-Mail: torsten.boeck@ikz-berlin.de

[4] Weierstrass Institute
Mohrenstr. 39
10117 Berlin
Germany
E-Mail: contact@wias-berlin.de

No. 3040
Berlin 2023

2010 *Physics and Astronomy Classification Scheme.* 73.21.La, 73.22.Dj, 81.10.Dn.

Key words and phrases. Quantum dots, electronic properties.

O.M. was funded by the Deutsche Forschungsgemeinschaft (DFG, German Research Foundation) under Germany's Excellence Strategy - EXC2046: MATH+ Berlin Mathematics Research Center (project IN-7).Fig. 6 was prepared using VMD. [12].

Edited by
Weierstraß-Institut für Angewandte Analysis und Stochastik (WIAS)
Leibniz-Institut im Forschungsverbund Berlin e. V.
Mohrenstraße 39
10117 Berlin
Germany

Fax: +49 30 20372-303
E-Mail: preprint@wias-berlin.de
World Wide Web: http://www.wias-berlin.de/

Energy level alignment of confined hole states in $InAs_{1-x-y}Sb_xP_y$ double quantum dots

Karen M. Gambaryan, Owen Ernst, Torsten Boeck, Oliver Marquardt

Abstract

We present a combined experimental and theoretical study of uncapped In(As,Sb,P) double quantum dots (DQD), suited for application in novel resonant tunneling nanodiods or single-photon nanooptical up- and down-converters in the mid-infrared spectral range. We provide details on the growth process using liquid-phase epitaxy (LPE), as well as on the characterization using atomic-force microscopy (AFM) and scanning electron microscopy (SEM). We find that most DQDs exhibit an asymmetry such that the two QDs of each pair have different dimensions, giving rise to correspondingly different quantum confinement of hole states localized in each QD. Based on these data, we have performed systematic simulations based on an eight-band $\mathbf{k} \cdot \mathbf{p}$ model to identify the relationship between QD dimensions and the energy difference between corresponding confined hole states in the two QDs. Finally, we have determined the strength of an applied electric field required to energetically align the hole ground states of two QDs of different dimensions in order to facilitate hole tunneling.

1 Introduction

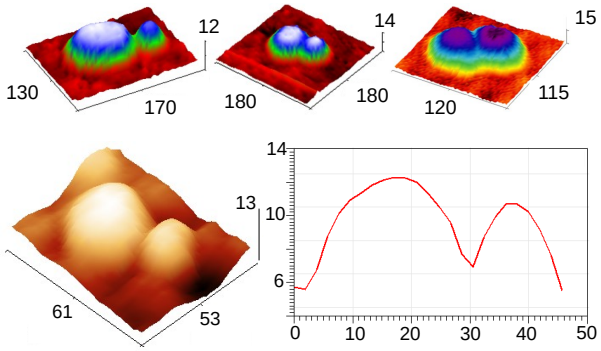

Figure 1: Top: AFM-images of typical In(As,Sb,P) DQDs grown on InAs by LPE. Bottom: A selected DQD (left) with its respective profile linescan (right). All dimensions are given in nm. (color online)

Semiconductor quantum dots (QDs) have attracted significant ongoing research interest for over two decades now, due to their unique physical features. [3]. A broad variety of potential applications of QDs ranges from single-photon sources, quantum computing and –cryptography, nanophotonics, or novel photodetectors. [21, 2] The In(As,Sb,P) material system appears best suited for the design of novel QD based systems for application in the mid-infrared spectral regime (3 to 5 μm), where the required QDs are obtained from Stranski-Krastanov growth [18]. The main driving force for QD nucleation in the Stranski-Krastanov growth mode is the lattice mismatch between the materials involved. If this mismatch is too large, however, the formation of point defects or dislocations becomes likely, leading to an overall reduction of the crystal quality and thus to a respective reduction of radiative recombination. These problems can be overcome if abrupt changes of the material and thus of the lattice constant at interfaces are replaced by smooth alloy gradients, which can be produced when growing heterostructures from the liquid phase using liquid-phase epitaxy (LPE) in a controlled and systematic manner. [1, 16, 13, 17]

DOI 10.20347/WIAS.PREPRINT.3040 Berlin 2023

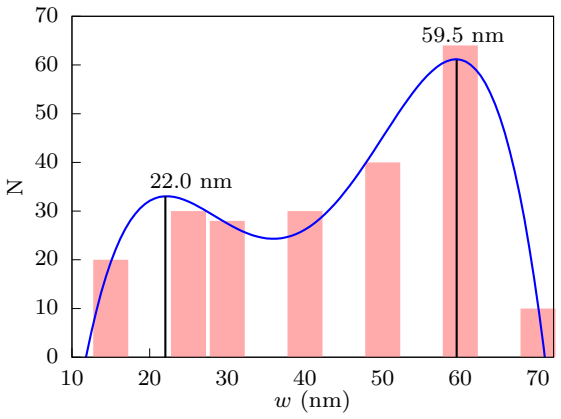

Figure 2: Histogram of the distribution of DQDs w.r.t. the distance w between the centers of the two QDs. The blue line is a 4^{th}-order polynomial fit as a guide-to-the eye with the two respective maxima being indicated as dashed black lines (color online).

The resulting nanostructures, In(As,Sb,P) graded-composition-QDs, represent type-II heterostructures where electrons are delocalized in the InAs substrate and hole states are confined in the Sb-rich areas at the top of the QDs.

We have dedicated a previous work to systematic investigations of not only the growth process and detailed characterization of In(As,Sb,P) graded-composition quantum dots, but also on the capabilities of theoretical approaches to compute their elastic and electronic properties. [10] We have shown that an eight-band $\mathbf{k}\cdot\mathbf{p}$ model for semiconductors in the zincblende phase represents an ideal tool for both a deeper understanding of observations in experiment and a theory-guided design process to identify suitable heterostructures for specific applications.

In the present work, we focus on novel, In(As,Sb,P)-based asymmetric double quantum dot systems for wavelength transfer based on hole tunneling. Double quantum dots (DQDs) have been successfully designed in the past, e.g. as artificial two-level systems [19], or for quantum computing. [6, 22] Due to the specific type II band profile of our DQDs, we consider them a unique, novel heterostructure for hole tunneling. While hole tunneling has been suggested for single quantum dots in the past, [14] and combined electron and hole tunneling has been studied in coupled InAs QDs before, [5], to our knowledge no theoretically predicted or experimentally realized design of coupled QDs exists in the mid-infrared regime that relies on hole tunneling for wavelength transfer.

2 Methodology and Results

2.1 Growth and characterization

The DQDs under consideration have been grown from the quaternary In-As-Sb-P liquid phase at T=580°C constant temperature (in contrary to traditional liquid phase epitaxy) on an undoped InAs(100) commercial substrate. According to the phase diagram of the In-As-Sb-P material system, the liquid phase composition was chosen to provide its corresponding supersaturation and $\sim$ 2.5% lattice mismatch between the wetting layer and the substrate as a mandatory driving force for the Stranski-Krastanow (S-K) growth mode. [18] The Mole fractions of the quaternary liquid phase were chosen as $X_{\text{InAs}} = 0.0197$, $X_{\text{InSb}} = 0.123$, and $X_{\text{InP}} = 1.8 \times 10^{-4}$. QD nucleation duration was equal to 30

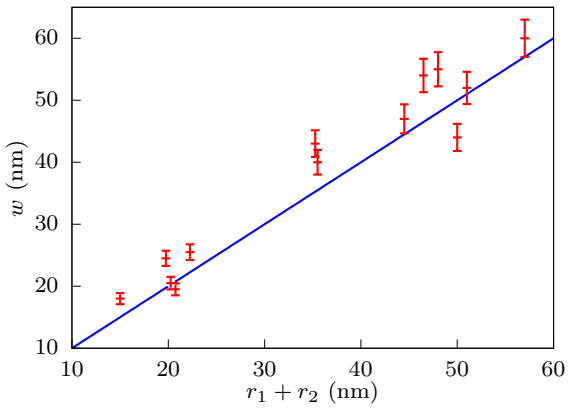

Figure 3: Measured distance w between the centers of the two QDs as a function of the sum of their radii, r_1 and r_2 (red). The blue line indicates the ideal case $w = r_1 + r_2$ (color online).

minutes. Other technological conditions are described in more detail in Ref. [10]. Surface characterization performed by atomic force (AFM-Asylum Research MFP-3D) and scanning electron microscopes (SEM-EDXA-FEI Nova 600-Dual Beam) show that most of the In(As,Sb,P) type-II uncapped QDs consist of single as well as laterally double QDs. The surface concentration of DQDs was up to two orders lower ($\sim 3{\times}10^7$ cm^{-2}) than that of single QDs ($\sim 5{\times}10^9$ cm^{-2}). The growth process was stopped at the initial stage of Ostwald ripening and coalescence to overcome further QD coarsening. AFM characterization reveals symmetric and nonsymmetric DQDs with the average ratio of radius to height of 3.2 ± 0.2 according to line-scan analysis. Oblique view AFM images of typical DQDs and the respective line-scan for one of them are presented in Fig. 1 and more examples can be found in the supplemental material. Based on AFM measurements and line-scans data we have analyzed the size distribution of the DQDs. Figure 2 shows the distribution of DQDs w.r.t. the distance w between the center of the two QDs. A 4$^{\text{th}}$-order polynomial fit as a guide-to the eye yields two peaks at 22.0 and 59.5 nm. The relation between the sum of the two radii of the QDs and their distance w allows to conclude that we observe in fact two adjacent, very close QDs rather than a single QD that exhibits two tips (cf. Fig. 3).

2.2 Simulations

Based on the microscopy data obtained above, we have performed a systematic study of the electronic properties of the DQDs for different dimensions using an eight-band $\mathbf{k}\cdot\mathbf{p}$ model for zincblende semiconductors. [7] Elastic properties and built-in piezoelectric potentials were obtained from linear elasticity theory and the Poisson equation, respectively, and are considered in the $\mathbf{k}\cdot\mathbf{p}$ model. [11, 8] The respective continuum models were employed within the plane-wave framework of the SPHInX library [4, 15, 9] and all required material parameters for InAs, $InAs_{1-x}Sb_x$, and $InAs_{1-y}P_y$ were taken from Ref. [20] without any modification. We have previously used a similar approach to compute the electronic properties of In(As,Sb,P) graded-composition quantum dots and found it to provide a surprisingly good agremeent with measured data. [10] All details required to reproduce our studies are given in the supplemental material.

As the relevant mechanisms for our study are of a quantum physical nature, our model DQD systems correspond to the smaller systems observed in experiment where energy quantization plays a more prominent role (e.g. $r_1 + r_2 < 30$ nm, cf. Fig. 3). In order to obtain a meaningful, systematic picture, we have fixed the aspect ratio of both QDs to the mean aspect ratio observed ($h/r = 0.3$) and the

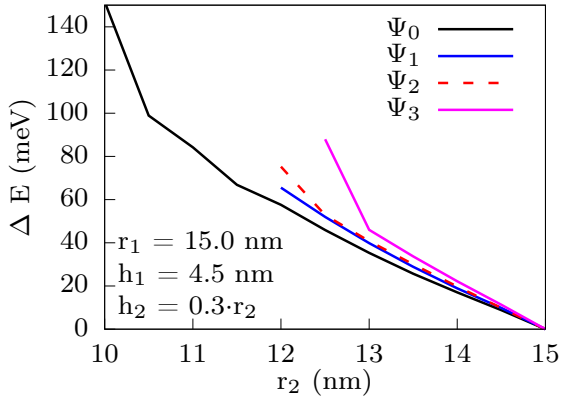

Figure 4: Energy difference between a hole state confined in QD2 and the corresponding state in QD1 as a function of the radius of QD2 for the hole ground state and the energetically following three excited states. (color online)

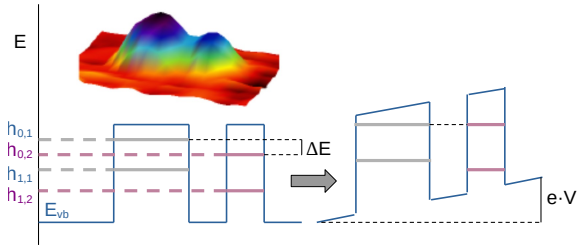

Figure 5: Schematic picture of valence band profile and confined hole states without (left) and with applied electric field to achieve an energetical alignment of the hole ground states of the two QDs (right). The inset shows an AFM image of a corresponding typical DQD. (color online)

radius of the larger QD to $r_1 = 15$ nm. The radius of the second QD, r_2, was then systematically varied between 5 and 15 nm and we have computed the energy difference between the hole ground state and first three excited states of the two QDs

$$\Delta E_i = E(\Psi^2_{\mathrm{ho,i}}) - E(\Psi^1_{\mathrm{ho,i}}) \quad \text{with } i = 0, 1, 2, 3$$

The energy differences between the hole ground state and the first three excited states' energies in the smaller QD and their counterparts in the larger one are shown in Fig. 4. Already for a radius of the smaller QD of $r_2 < 12$ nm, the index of the respective state in QD2 exceeds the total number of states computed in the DQD system (100 states) so that we follow only the ground state below this radius. The energy difference of the ground state and the excited states here is approx. 60 to 75 meV for $r_2 = 12$ nm. The energy difference between the ground states of the two QDs then increases further with reducing r_2 and exceeds 100 meV for $r_2 < 10.5$ nm.

In order to align the ground states of the two QDs to facilitate hole tunneling, the above energy difference can be overcome by applying an external electric field to the QDQs, as outlined schematically in Fig. 5. In the next step, we have therefore simulated the influence of an external electric field by adding a respective electrostatic potential to our simulation of the DQD system. Figure 6 shows the electric field required to achieve an energetical alignment of the hole ground states of the two QDs as a function of the radius of the smaller QD, r_2. We find that an alignment of the hole ground states can be achieved even for cases where the second QD has less than half the radius and diameter of

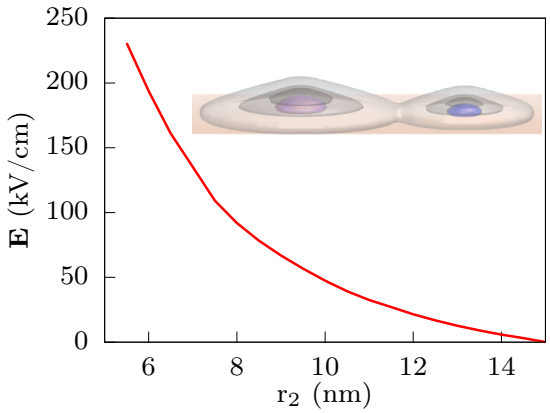

Figure 6: Electric field required to achieve an energetic alignment of the hole ground state of QD1 and QD2 as a function of QD2s radius. The inset shows a 3D image of a DQD consisting of a smaller ($r_2 = 10\ nm$) and a larger ($r_1 = 15\ nm$) dot with the hole ground state charge density of each dot in purple and blue. Grey isosurfaces indicate the Sb content (5, 10, 15%). (color online)

the larger one. For 10 nm $< r_2 <$ 15 nm, Such an alignment is achieved using fields of less than 50 kV/cm. With $r_2 < 7.5$ nm, the required field exceeds 100 kV/cm, which is still experimentally feasible.

3 Summary

We have presented a novel, In(As,Sb,P)-based DQD heterostructure consisting of two QDs of different size grown in a controlled, efficient and inexpensive manner from the liquid phase. Using the characteristic properties of these nanostructures as obtained from detailed AFM and SEM measurements, we have performed systematic simulations of their electronic properties using an eight-band $\mathbf{k} \cdot \mathbf{p}$ model that was in the past found to provide a highly accurate description of LPE-grown In(As,Sb,P) QDs. We have computed the energy difference between the hole ground states of the two QDs as a function of the size of the smaller dot, and determined the required electric field to achieve an energetical alignment of these two states. The resulting fields are in the order of a few tens to 200 kV/cm and thus experimentally realizable.

The DQDs reported in our manuscript can potentially be employed for wavelength conversion in the mid-infrared spectral range in both directions, for transistors based on hole tunneling, or for applications in energy harvesting.

References

[1] Z. Alverov, V. Andreyev, S. Konnikov, V. Larionov, and B. Pushny. *Kristall und Technik*, 11:1013, 1976.

[2] P. Bhattacharya, X. H. Su, S. Chakrabarti, G. Ariyawansa, and A. G. U. Perera. *Applied Physics Letters*, 86(19):191106, 2005.

[3] D. Bimberg, M. Grundmann, and N. Ledentsov. *Quantum Dot Heterostructures*. Wiley, 1999.

[4] S. Boeck, C. Freysoldt, A. Dick, L. Ismer, and J. Neugebauer. *Computer Phys. Commun.*, 182:543, 2011.

[5] A. S. Bracker, M. Scheibner, M. F. Doty, E. A. Stinaff, I. V. Ponomarev, J. C. Kim, L. J. Whitman, T. L. Reinecke, and D. Gammon. Engineering electron and hole tunneling with asymmetric inas quantum dot molecules. *Appl. Phys. Lett.*, 89:233110, 2006.

[6] D. P. Di Vincenzo. Double quantum dot as a quantum bit. *Science*, 309:2173, 2005.

[7] P. Enders, A. Bärwolff, M. Woerner, and D. Suisky. *Phys. Rev. B*, 51:16695–16704, 1995.

[8] V. A. Fonoberov and A. A. Balandin. *J. Appl. Phys.*, 94:7178, 2003.

[9] C. Freysoldt. Sphinx repository. *sxrepo.mpie.de*.

[10] K. M. Gambaryan, T. Boeck, A. Trampert, and O. Marquardt. Nucleation chronology and electronic properties of $InAs_{1-x-y}Sb_xP_y$ graded composition quantum dots grown on an InAs(100) substrate. *ACS Applied Electronic Materials*, 2(3):646–650, 2020.

[11] M. Grundmann, O. Stier, and D. Bimberg. Inas/gaas pyramidal quantum dots: Strain distribution, optical phonons, and electronic structure. *Phys. Rev. B*, 52:11969–11981, Oct 1995.

[12] W. Humphrey, A. Dalke, and K. Schulten. Vmd: Visual molecular dynamics. *Journal of Molecular Graphics*, 14(1):33 – 38, 1996.

[13] A. Kumar and P. Dutta. *Journal of Crystal Growth*, 310(7):1647 – 1651, 2008.

[14] E. Leobandung, L. Guo, and S. Y. Chou. Single hole quantum dot transistors in silicon. *Appl. Phys. Lett.*, 67:2338, 1995.

[15] O. Marquardt, S. Boeck, C. Freysoldt, T. Hickel, S. Schulz, J. Neugebauer, and E. P. O'Reilly. *Comp. Mat. Sci.*, 95:280, 2014.

[16] M. G. Mauk, A. N. Tata, and J. A. Cox. *Journal of Crystal Growth*, 225(2):236 – 243, 2001. Proceedings of the 12th American Conference on Crystal Growth and Epitaxy.

[17] A. Singh, A. K. Shukla, and R. Pal. *AIP Advances*, 5(8):087172, 2015.

[18] I. Stranski and L. Krastanow. *Math. Naturwiss.*, 146:797, 1938.

[19] W. G. Van der Wiel, T. Fujisawa, S. Tarucha, and L. P. Kouwenhoven. A double quantum dot as an artificial two-level-system. *Jpn. J. Appl. Phys*, 40:2100, 2001.

[20] I. Vurgaftman, J. R. Meyer, and L. R. Ram-Mohan. *J. Appl. Phys.*, 89:5815, 2001.

[21] J. Wu, D. Shao, V. G. Dorogan, A. Z. Li, S. Li, E. A. DeCuir, M. O. Manasreh, Z. M. Wang, Y. I. Mazur, and G. J. Salamo. *Nano Letters*, 10(4):1512–1516, 2010.

[22] H. Zheng, J. Zheng, and R. Berndt. A minimal double quantum dot. *Scientific Reports*, 7:10764, 2017.